

Dependence of radiative stabilization on the projectile charge state after double-electron-transfer processes in slow, highly charged ion-molecule collisions

Franciszek Krok,^{*} Inga Yu. Tolstikhina, Hiroyuki A. Sakaue, Ichihiko Yamada, Kazumoto Hosaka,[†] Masahiro Kimura,[‡] Nobuyuki Nakamura,[§] Shunsuke Ohtani,[§] and Hiroyuki Tawara

National Institute for Fusion Science, Nagoya 464-01, Japan

(Received 13 February 1997)

We have measured the radiative stabilization probabilities after double-electron-transfer processes in slow (1.5q keV) $I^{q+} + \text{CO}$ collisions in the charge-state regime $8 \leq q \leq 26$ by using the charge-selected-projectile-recoil-ion-coincidence method. It was found that the radiative stabilization probabilities P_{rad} , defined as $P_{\text{rad}} = T_{\text{DC}} / (T_{\text{DC}} + A_{\text{DC}})$ (T_{DC} is true double capture, and A_{DC} autoionizing double capture), increases from about 1% at the lowest charge up to about 10% at the highest charge as the charge state of the projectile increases. A model is proposed which can explain such a feature, by incorporating a slight modification of the initial population of the transferred levels in the projectile predicted in the extended classical over-barrier model. Based upon the present model, theoretical radiative and autoionization decay rates have been calculated, using the Cowan code. Fairly good agreement between the measured and calculated results has been obtained. [S1050-2947(97)03312-X]

PACS number(s): 34.70.+e

I. INTRODUCTION

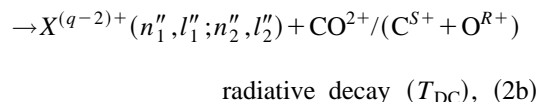
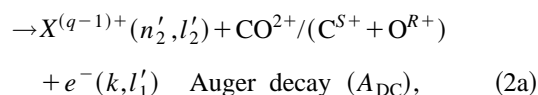
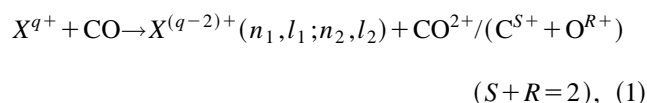
In low-energy collisions of highly charged ions (HCI's) with atoms, electron transfer is the dominant reaction channel. In such collisions, several target electrons can be transferred into multiply excited Rydberg levels of HCI's [1]. The occupied Rydberg states of the transferred electrons can be reasonably predicted with the extended classical over-barrier model (ECBM) [2]. The stabilization processes of the multiply excited Rydberg states occurring in the projectile ions are very important, not only for the basic atomic collision physics but also, for example, for studying the composition of plasmas in astrophysical objects or for the plasma diagnostics in thermonuclear plasmas.

In the past few years processes occurring in the projectile ions after two-electron transfer have been a subject of the intensive studies, both experimentally and theoretically [3]. The doubly excited states formed are stabilized through the ejection of an electron (Auger decay) or photons (radiative decay). The stabilization of both electrons without changing the charge state of the projectile after two electron transfer (the true double capture T_{DC}) is explained either by direct stabilization of symmetrical or quasisymmetrical electron configurations created during collisions [4,5,6] or by a rearrangement of transferred electrons (transfer to asymmetric Rydberg states) in the field of the outgoing recoil ion (the so-called post-collision interaction) [7]. Another mechanism feeding asymmetrical states, so-called correlated double

electron capture, was proposed by Stolterfoht *et al.* [8]. These highly asymmetric Rydberg states, especially with large angular momentums are well known to be stabilized mainly radiatively [9]. On the other hand, symmetrically or quasisymmetrically populated Rydberg states are known to be dominantly autoionizing (the autoionizing double capture A_{DC}). A strong influence of the core electron configuration of the projectile on the radiative stabilization of the excited Rydberg states has also been reported [10,11].

It now seems interesting to investigate how much the stabilization of the excited Rydberg states formed in collisions of HCI's with a molecular target differs from that formed in collisions with atomic targets. On the other hand, such an experiment involving interactions between HCI's and molecules is one of the effective methods of studying the dissociation of multiply charged molecular ions [12,13].

The products of interaction processes of HCI's with a molecular target (for example, CO) after two electron transfer process can be described as follows:



where n_i, l_i and n'_i, l'_i, n''_i, l''_i , ($i=1$ and 2) are the principal and orbital momentum quantum numbers of the transferred electrons before and after the stabilization processes, respectively, and k is the wave vector of the electron in continuum. The molecules after loss of electrons during collisions with HCI's can remain stable (CO^{2+}) or dissociate into fragmented ions $\text{C}^{S+} + \text{O}^{R+}$. The kinetic energy of the frag-

^{*}Permanent address: Institute of Physics, Jagiellonian University, ul. Reymonta 4, 30-059 Krakow, Poland.

[†]Permanent address: The Graduate University for Advanced Studies, Nagoya 464-01, Japan.

[‡]Permanent address: Kochi University of Technology, Tosa-Yamada, Kochi 782, Japan.

[§]Permanent address: University of Electro-Communications, Chofu 182, Japan.

mented ions can also provide more information about the dynamic of the collision, which is another interesting topic presently being pursued [13].

In this paper, we investigate the dependence of the radiative stabilization of high Rydberg states after double-electron-transfer processes on the charge state of the projectile in $1.5q$ keV I^{q+} ($8 \leq q \leq 26$) – CO collisions. It is found that radiative stabilization probabilities, defined as ratios of radiative transition rates to total (radiative plus Auger decay) rates, increase as the charge of the projectile ions increases. To explain the observed features, a model in which, at the present collision energy, the transfer of two electrons occurs dominantly into the highest possible orbital momentum states l for a given level n is proposed.

II. EXPERIMENT

We measured the charge-state distributions of the scattered ions in coincidence with the charge-selected recoil ions. The experimental procedures have been reported previously [14]. Briefly, highly charged iodine ions produced in an electron-beam ion source, called NICE [15], were extracted at the energy of $1.5q$ keV. The incident I^{q+} ions were mass charge separated by a magnet, and introduced through an entrance aperture 0.5 mm in diameter into a collision area. The scattered $I^{(q-j)+}$ ($j=1$ and 2) ions which captured one- or two-electrons were simultaneously detected with a position-sensitive detector (PSD) after charge analyzing in a 127° electrostatic analyzer. The recoil ions were extracted from the collision area by the weak electric field (10 V/cm), and their mass-charge states were determined through a time-of-flight spectrometer [16]. A microchannel plate (MCP) recoil ion detector provided the start pulse to a time-to-amplitude converter which was stopped by the PSD signal. The flight times of the recoil ions were typically of a few microseconds. The target density was kept low enough to suppress multiple collisions efficiently, but high enough to obtain reasonable count rates. During the measurements the pressure of the target gas in the collision chamber was measured to be about 4.0×10^{-7} Torr. The contribution of multiple collisions is described in detail in Sec. III.

III. EXPERIMENTAL RESULTS

We determined the radiative stabilization probabilities of the projectile iodine ions after double-electron-transfer processes by using the coincidence measurements between the charge-selected scattered ($I^{(q-2)+}$ and $I^{(q-1)+}$) ions and the metastable molecular recoil CO^{2+} ions. Experimentally, the radiative stabilization probability $P_{\text{rad}} = T_{\text{DC}} / (T_{\text{DC}} + A_{\text{DC}})$ is obtained as the ratio of the amount of $I^{(q-2)+}$ ion counts in coincidence with the CO^{2+} ions to all of projectiles measured coincidentally with the recoil CO^{2+} ions. In the present work, where a weak extraction field was used, only the parent molecular ions CO^+ and CO^{2+} were collected, mean-

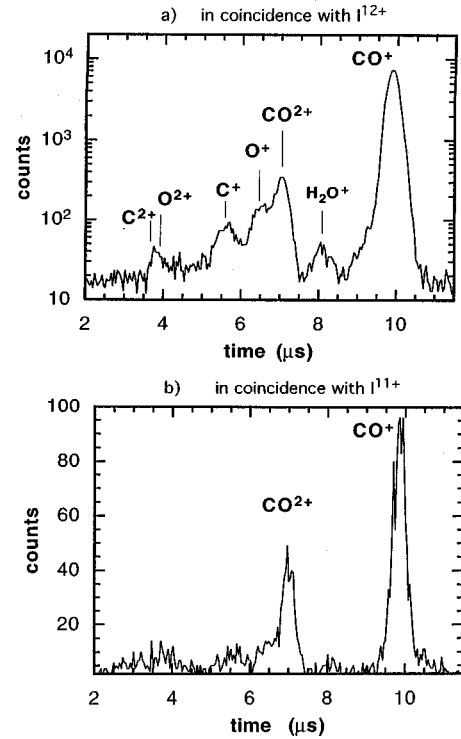
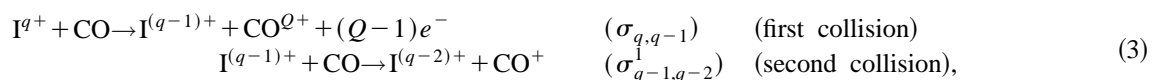


FIG. 1. Typical TOF spectra of recoil ions produced in 19.5-keV $I^{13+} + \text{CO}$ collisions, measured in coincidence with I^{12+} (a) and I^{11+} (b) ions, with an extraction field of 10 V/cm.

while, not all of the fragmented ions C^{S+} and O^{R+} were collected because of their large initial kinetic energy. Only these fragmented ions produced within a cone aligned toward the MCP were detected.

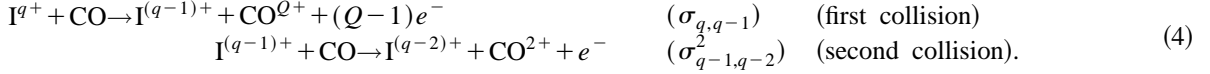
Figure 1 presents typical time-of-flight spectra for $I^{13+} + \text{CO}$ collisions. In Fig. 1(a) we show the CO^+ and CO^{2+} peaks in coincidence with the one-electron-captured I^{12+} ions, which are due to the single-electron-capture (S_{EC}) and autoionizing double-capture (A_{DC}) processes, respectively. The fragmented O^+ and C^+ ion peaks correspond to the break-up of molecular ions. Previous investigations [17,18] reported that, for both slow and fast collisions, the produced molecular CO^{Q+} ions predominantly break up into the fragmented ions C^{R+} and O^{S+} ($R+S=Q$). The fact that the positions of the CO^{2+} and O^+ ion peaks are not in the order of the m/q ratio in the present spectrum is a consequence of the large initial energy of the fragmented O^+ ions; meanwhile CO^{2+} ions have small initial kinetic energy. In the spectrum in coincidence with the I^{11+} ions [Fig. 1(b)], the CO^{2+} peak corresponds to the true double capture (T_{DC}), and the CO^+ peak is due to double collisions (D_C). The peak areas were determined through fitting a Gaussian curve to the spectrum peaks.

Special care has been taken to estimate the contribution of double collisions to the observed results. The double collisions (D_C peak) can be due to the following process:

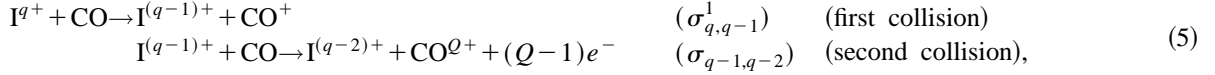


where $\sigma_{q,q-j}^i$ is the cross section for capture of j electrons by a projectile with the primary charge state q when i electrons are removed from a target, and $\sigma_{q,q-j}$ is the total cross section for capture of j electrons. In process (3), one electron is captured into the projectile ion in the first collision before reaching the target region. Then this one-electron captured projectile ion collides with another target molecule and captures the second electron, producing a single charged recoil ion which is extracted into the recoil ion detector and measured in coincidence with the two-electron captured projectile ion.

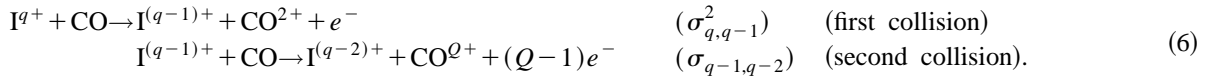
The following double collisions can contribute to the T_{DC} peak:



Similarly the following collision processes, where the first collision occurs in the extraction area and the second collision occurs outside the extraction area can contribute to the D_C peak:



and to the T_{DC} peak,



It has been assumed in the present pressures of the target gas that only one collision [the second in the processes (3) and (4) and the first in processes (5) and (6)] occurs in the extraction area, and the other outside the extraction region. This seems to be reasonable as the ratio of the length of the collision chamber to the length of the extraction area of about 6 mm is about 75 in the present experimental setup. Furthermore, as the distance from an entrance into the collision chamber to the extraction area is about three times longer than the distance from the extraction area to an exit of the collision chamber, processes (5) and (6) should make minor contributions to the total double collisions.

Therefore it is assumed that the double collisions are mainly due to process (3), and that the contribution of double collisions to the measured T_{DC} is mostly due to process (4). Under these assumptions, the percentage of double collisions (D_C^P) has been estimated as the ratio of intensities of the measured D_C peak to the S_{EC} peak multiplied by the ratio of cross sections for the first and second collisions:

$$D_C^P = \frac{D_C}{S_{EC}} \frac{\sigma_{q,q-1}}{\sigma_{q-1,q-2}^1}. \quad (7)$$

Finally, the corrected value of T_{DC} (T_{DC}^C) has been obtained by subtracting from the measured T_{DC} the measured A_{DC} multiplied by the percentage of double collisions and the ratio of cross sections for the second and first collisions (4):

$$T_{DC}^C = T_{DC} - (A_{DC} D_C^P) \frac{\sigma_{q-1,q-2}^2}{\sigma_{q,q-1}} = T_{DC} - A_{DC} \frac{D_C}{S_{EC}} \frac{\sigma_{q-1,q-2}^2}{\sigma_{q-1,q-2}^1}. \quad (8)$$

To perform this correction, the ratio $\sigma_{q,q-1}^2/\sigma_{q,q-1}^1$ must be known. This ratio for the present collision system is expected to be 15% from the measured total cross sections for capture electrons (σ_q) for the I^{q+} ions of the energy of 1.5q keV [19]. Similar results for slow Ar^{8+}/N_2 collisions were reported by Remscheid *et al.* [13]. In order to make a more

precise estimation of this ratio, values of the σ_q^1 and σ_q^2 for collisions of $I^{q+} + Ar$ at an energy of 1.5q keV have been used [20], where σ_q^i is the absolute cross section for removal of i electrons from a target by a projectile of the charge state q . In our separate work, the total cross section (σ_q) and cross section for one-electron capture ($\sigma_{q,q-1}$) for I^{q+} in collisions with Ar have been found to be almost the same as those for collisions with the CO target. In this case this ratio was estimated to be in the range of 45–50% for $8 \leq q \leq 26$. It is an upper limit of the ratio because of σ_q^1 ($\sigma_q^1 = \sigma_{q,q-1}^1$ as no direct ionization is expected at the present energy) and σ_q^2 ($\sigma_q^2 > \sigma_{q,q-1}^2$) were used to estimate it. To determine a fraction of the primary beam captured electrons in collisions with background gases, measurement without the target was performed. This fraction was estimated to be below 1%. The total correction for the double collisions and an interaction with background gases in the present work is 1–4%.

In Fig. 2 we show the measured radiative stabilization ratios P_{rad} for I^{q+} ions colliding with a CO target as a function of the projectile charge q , together with those for rare gasses (Ne, Ar, Kr, Xe). Clearly there is practically no difference in P_{rad} whether the targets are molecules or atoms. This comparison confirms that the radiative stabilization occurring in the projectile does not depend on the target states. The observed P_{rad} gradually increases from about 1% up to about 10% as the charge of the projectile increases, though some structures are seen, as discussed below. The behavior of P_{rad} can be divided into three regions corresponding to the successive appearance of vacancies in the outer subshells, with particular core-electron configurations of the projectile. For the first region ($q=8-17$), the outer electrons belong to the 4d subshell of the projectile with the $(1s^2 \dots 4p^6)$ core configuration. The maximum of P_{rad} in this region at $q=13$ ($4d^4$) corresponds to a case where the number of electrons and vacancies in the subshell is almost the same. This feature is more clearly seen in the second region (q

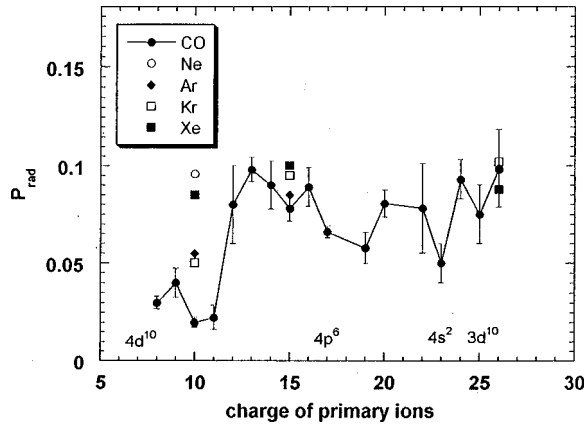


FIG. 2. The measured radiative stabilization as a function of the projectile charge state for the $I^{(q-2)+**}$ ions after two-electron transfer from CO (●) and rare-gas targets (Ne—○; Ar—◆; Kr—□; Xe—■; data for $q=10$ and 15 from Ref. [20], for $q=26$ from Ref. [21]) at a collision energy of $1.5q$ keV. The full outer subshells of the projectile core are indicated.

$=17-23$), where the maximum of P_{rad} at $q=20$ corresponds to a case where three electrons and three vacancies are present in the outer $4p$ subshell. Similarly, in the third region ($q=23-25$), a maximum is observed at $q=24$ for which the outermost $4s$ subshell is half-filled (one electron). The last data point at $q=26$ (the highest value of the P_{rad}) corresponds to a case where a new shell with $n=3$ ($3d^9$) is open.

It should be noted that the present results are in general agreement with the previous measurements of radiative stabilization made in slow $\text{Xe}^{q+}-(\text{Xe}, \text{He})$ collisions [10,22], as shown Fig. 3, though those for He show slight variations.

Similar structures in the dependence of P_{rad} on the charge state of projectiles were also observed by Ali *et al.* [11] in $\text{Kr}^{q+}-\text{Ar}$ collisions. To explain the structures, Ali *et al.* proposed a model based on the assumption that both the core structures of the projectile and the asymmetry of the transferred levels play an important role in the radiative stabilization processes. They assumed that a significant fraction of highly asymmetric Rydberg states ($6l, 20l'$) with high orbital momentum states (l, l') is populated during the double-electron-transfer process. Further, they assumed that if these doubly excited states survive autoionization until one electron undergoes cascade down the yrast chain [a chain of the

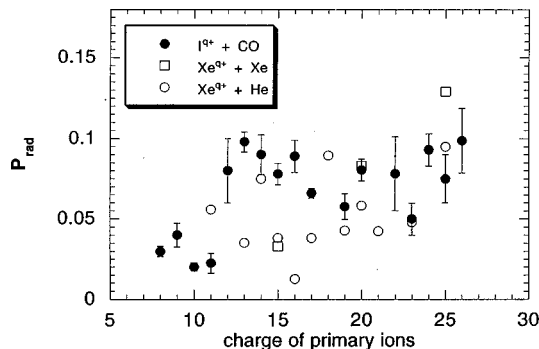


FIG. 3. Comparison between the present measured P_{rad} for $I^{q+} + \text{CO}$ (●) collisions, and results obtained for collisions of Xe^{q+} with Xe (□ from Ref. [10]) and with He (○ from Ref. [22]).

radiative transitions of an electron in the quantum state ($n, l=n-1$) through $\Delta n = -1$ or 0 and $\Delta l = -1$], the radiative stabilization depends on whether the last step of the cascade will be $\Delta n = -1$ (e.g., $3d-2p$) or $\Delta n = 0$ (e.g., $2p-2s$) transitions. For a system created by the core configuration and the down-going electron in the last step of the yrast chain, they found terms which are not metastable against the radiative decay. The radiative stabilization probability was then defined as the ratio of the sum of statistical weights (e.g., $2J+1$ in the $L-S$ coupling scheme $^{2S+1}L_J$, where L, S , and J are the total orbital, spin, and total angular momentum quanta, respectively) of these nonmetastable terms to the sum of statistical weights of all possible terms created.

In the model presented below we took into account all steps of the cascades as, at every step, there is a competition between the radiative and autoionization processes. We noted through extensive calculations of the radiative and autoionization decay rates that, in contrast to a model proposed by Ali *et al.* the first step of the cascades, instead of the last one, is more crucial for the final radiative stabilization process.

IV. MODEL AND CALCULATIONS

In the present model our assumptions are as follows.

(a) For the present velocities of the projectile ≈ 0.1 a.u., electron transfer occurs dominantly into the highest possible orbital momentum states l for a given level n (that is $l=n-1$). It is well known that the l distributions are strongly dependent upon the ion-target combinations. In fact, there is no clear evidence that for the present velocities the highest l states are the most dominant. In particular, there are no general rules on the l distributions for highly charged ion collisions like that in the present work, where the electron is transferred into high n states. But in a number of collision systems higher l states are more populated for relatively low Z ions (Z is the atomic number of the projectile ion), as recent precise multichannel atomic-orbital calculations have also shown [23,24,25]. That is why we make this assumption.

(b) During the radiative cascade of an electron which was transferred into the inner shell (n_2, l_2), another electron which was transferred into the outer shell (n_1, l_1) remains at its original state. The cascade is finished when going down throughout the yrast chain the electron (n_2, l_2) forms the ground state of the ion $I^{(q-1)+}$, with $(Z-q)$ core electrons in the projectile I^{q+} .

(c) For the autoionization process where one (outer) electron (n_1, l_1) is ejected to the continuum (k, l'_1), while the second (inner) electron (n_2, l_2) (naturally $n_2 \leq n_1$) goes down to the energetically allowed level (n'_2, l'_2), we consider only channels with the highest decay probabilities. It is expected from the selection rule for the autoionization process, namely, $\Delta L=0$, where L is the total orbital momentum quantum number of the ion, that the autoionization decay rates are highest when the differences of the l for both electrons satisfy the following condition [26]:

$$\Delta l_1 + \Delta l_2 = 0 \quad (\Delta l_i = l'_i - l_i). \quad (9)$$

Furthermore, the maximum autoionization probability is expected to occur when $\Delta l_1 = \Delta l_2 = 0$, namely, when l for both electrons is the same before and after autoionization. This conclusion is supported by the following calculation.

The autoionization level width for the two-electron system $(n_1, l_1; n_2, l_2)$, where one of the electrons (n_1, l_1) goes to continuum (k, l'_1) and the other to the (n'_2, l'_2) state, is given by [27]

$$\Gamma(n_1 l_1 n_2 l_2; LS) = \frac{2\pi}{k} \sum_{l'_1 n'_2 l'_2} \left| \left\langle n_1 l_1 n_2 l_2 LS \left| \frac{1}{r_{12}} \right| k l'_1 n'_2 l'_2 LS \right\rangle \right|^2, \quad (10)$$

where k is the wave vector of the electron in continuum. The Coulomb matrix element in Eq. (10) can be expressed as

$$\begin{aligned} & \left\langle n_1 l_1 n_2 l_2 LS \left| \frac{1}{r_{12}} \right| k l'_1 n'_2 l'_2 LS \right\rangle \\ &= \sqrt{(2l_1+1)(2l_2+1)(2l'_1+1)(2l'_2+1)} \\ & \times \sum_l (-1)^{L+l+(1/2)(l_1+l'_1-l_2-l'_2)} \\ & \times \left[\begin{Bmatrix} l_1 l_2 L \\ l'_2 l'_1 l \end{Bmatrix} P_l(n_1 l_1 n_2 l_2; n'_2 l'_2 k l'_1) \right. \\ & \left. + (-1)^{L+S} \begin{Bmatrix} l_1 l_2 L \\ l'_1 l'_2 l \end{Bmatrix} P_l(n_1 l_1 n_2 l_2; k l'_1 n'_2 l'_2) \right], \quad (11) \end{aligned}$$

where

$$P_l(n_1 l_1 n_2 l_2; k l'_1 n'_2 l'_2) = (ll'_1 l_1)(ll'_2 l_2) R_l(n_1 l_1 n_2 l_2; k l'_1 n'_2 l'_2). \quad (12)$$

$(ll'_1 l_1)$ and $(ll'_2 l_2)$ in Eq. (12) are the $3j$ symbols, and $R_l(n_1 l_1 n_2 l_2; k l'_1 n'_2 l'_2)$ is the Coulomb radial integral with one continuous parameter given by

$$\begin{aligned} R_l(n_1 l_1 n_2 l_2; k l'_1 n'_2 l'_2) &= \int_0^\infty dr_1 r_1^2 \int_0^\infty dr_2 r_2^2 V_l(r_1, r_2) \\ & \times R_{n_1 l_1}(r_1) R_{n_2 l_2}(r_2) R_{k l'_1}(r_1) \\ & \times R_{n'_2 l'_2}(r_2), \end{aligned}$$

where

$$V_l(r_1, r_2) = \theta(r_1 - r_2) \frac{r_2^l}{r_1^{l+1}} + \theta(r_2 - r_1) \frac{r_1^l}{r_2^{l+1}},$$

and $V_l(r_1, r_2)$ is the operator of the electrostatic interaction between two electrons and nucleus, $R_{n_i}(r)$ is the hydrogenic radial function, r_i ($i=1$ and 2) is the distance between the i th electron and the nucleus and $\theta(r_1 - r_2)$ is the theta function.

The numerical calculations of Eq. (11), with fixed initial states of electrons $(n_1, l_1; n_2, l_2)$ and various allowed final states $(k, l'_1; n'_2, l'_2)$, lead to the conclusion that the values of the radial integrals depend strongly on the final states of the

electrons, while the values of $3j$ symbols do not change significantly when the final states of electrons change.

In order to define which final states of electrons will result in the maximum values of the Coulomb radial integral, we consider an integral written in the following form:

$$R_l(n_1 l_1 n_2 l_2; k l'_1 n'_2 l'_2) = \int_0^\infty dr_2 r_2^2 R_{n_2 l_2}(r_2) R_{n'_2 l'_2}(r_2) F_l(r_2), \quad (13)$$

where

$$F_l(r_2) = \int_0^\infty dr_1 r_1^2 V_l(r_1, r_2) R_{n_1 l_1}(r_1) R_{k l'_1}(r_1).$$

It can be easily seen from Eq. (13) that this integral has a maximum value when the overlapping of two hydrogenic radial functions $R_{n_2 l_2}(r_2)$ and $R_{n'_2 l'_2}(r_2)$ is maximum.

Here we consider an electron moving in the central field with the potential

$$U_l(r) = -\frac{Z}{r} + \frac{l(l+1)}{r^2}, \quad (14)$$

where l is the orbital quantum number of the electron. This potential provides the electronic states described by the radial functions with a given orbital quantum number l and different radial quantum numbers $n_r = n - l - 1$ (n is the principal quantum number), that is, the number of nodes of the radial function. If the electronic state is described by the orbital momentum l' , the electron moves in a potential well $U_{l'}(r)$, whose minimum is shifted with respect to the minimum of the potential well $U_l(r)$. When the difference between l' and l is larger, the shift of the minima becomes larger, and the overlapping of the radial functions becomes smaller. The largest overlapping of two radial functions $R_{n_2 l_2}(r_2)$ and $R_{n'_2 l'_2}(r_2)$ is achieved clearly when the initial and final states of the electron are supported by the same potential well, i.e., $l_2 = l'_2$. Figure 4 shows the hydrogenic radial functions $R_{n_2 l_2}(r_2)$ and $R_{n'_2 l'_2}(r_2)$ for the following cases: $n_2 = 3$, $n'_2 = 2$, and $l_2 = l'_2 = 1$ [Fig. 4(a)], and $n_2 = 3$, $n'_2 = 2$, and $l_2 = 2$, $l'_2 = 1$ [Fig. 4(b)]. Numerical calculations show that the autoionization probability for $\Delta l_1 = \Delta l_2 = 0$ is at least one order of magnitude larger than that for other values of Δl_i ($i=1$ and 2) allowed by the selection rule for the autoionization process [26].

To understand the effect of the assumptions mentioned above for the autoionization decay processes, let us now consider the possible terms created during the electron-transfer process. For example, for the incident I^{7+} with the core electron configuration $1s^2 \dots 4d^{10}$, two electrons are transferred into the levels $n_1 = 6$ and $n_2 = 5$, predicted by the ECBM, with the highest l , namely, $l_1 = 5$ and $l_2 = 4$, respectively. For this electronic configuration there are $2(2l_2 + 1) = 18$ ($l_2 < l_1$) possible terms (from P to M states) in the ion under consideration, according to the rule $|l_1 - l_2| < L < |l_1 + l_2|$. The ejection of the electron from the transferred level $n_1 = 6$ is energetically permitted only when the second electron goes down to the lower level $n'_2 = 4$, i.e., $\Delta n_2 = -1$ and, according to Eq. (9), the autoionization probability becomes largest when $\Delta l_1 = 1$ and $\Delta l_2 = -1$. This means that for $2|2\Delta l_2| = 4$ terms (namely, for the P and D terms), autoion-

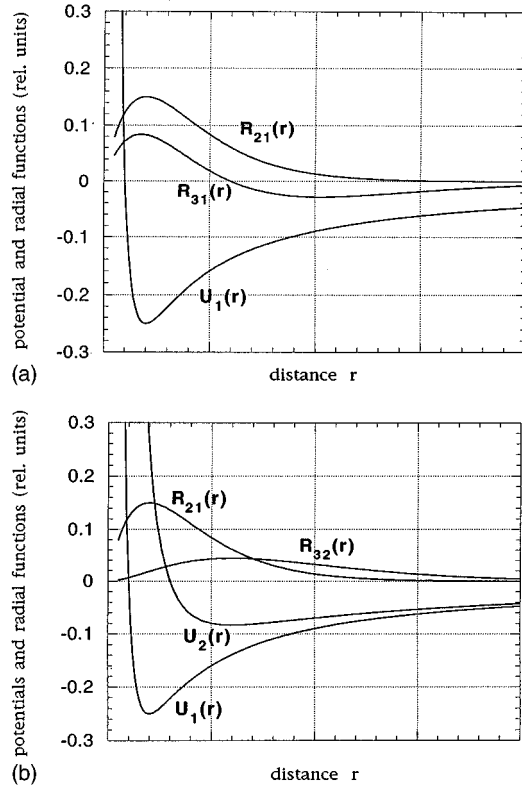


FIG. 4. Examples of the hydrogenic radial functions $R_{nl}(r)$ of two electrons (a) with the same orbital momentum quantum number l and (b) with the different l as a function of the distance between the electron and nucleus.

ization is prohibited, due to the selection rule, because for the new electron configuration with one electron in the continuum there are only $2(2l'_2 + 1) = 14$ ($l'_2 < l'_1$) terms (namely, from F to M), resulting from $|l_1 - l_2 - 2\Delta l_2| < L' < |l_1 + l_2|$ [see Eq. (9)], among which the initial electron configuration can decay during autoionization. For the higher charge state of the projectiles, the electron is transferred into higher n , where the energy difference between the neighboring n levels becomes smaller. Therefore, in order that the autoionization be allowed, $|\Delta n_2|$ as well as $|\Delta l_2|$ becomes larger, and, thus, for more terms created during the double electron transfer processes, the autoionization is prohibited.

Based on the model, we calculated the radiative stabilization probabilities, using the Cowan code [28]. For every i th term (i is a successive, possible term $^{2S+1}L_J$) of the configuration: the core electron configuration of the projectile and two transferred electrons, created in collisions, we calculated the radiative (A_r^i) and autoionization (A_a^i) decay rates and obtained the radiative stabilization probability as follows:

$$p_{\text{rad}}^i = \frac{A_r^i}{A_r^i + A_a^i}. \quad (15)$$

We assumed that each of these terms is populated statistically (with the statistical weight W_i). In the L - S coupling scheme, $W_i = 2J_i + 1$, where J_i is the total angular momentum of the i th term. Then the radiative stabilization of a given configuration in the k th step of the radiative cascades was obtained in the following way:

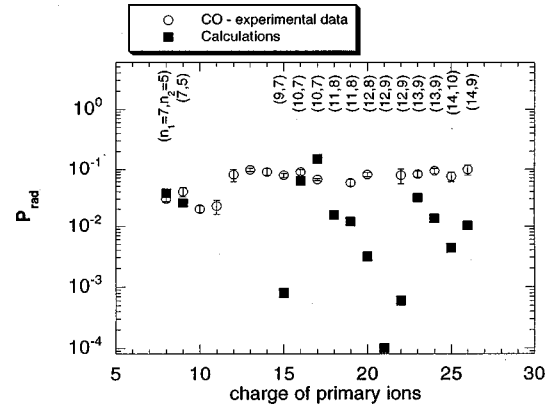


FIG. 5. The measured and calculated radiative stabilization after double-electron-transfer processes vs the initial charge of the projectile ions. The transferred projectile levels (n_1, n_2) predicted by the ECBM are shown in the figure, and used in the present calculations. n_i ($i = 1$ and 2) presented here are the highest integer numbers satisfying an inequality $n_i \leq n_{\text{ECBM}}$ as the occupied levels n_{ECBM} predicted by the ECBM are the real numbers.

$$P_{\text{rad}}^k = \frac{\sum_i W_i P_{\text{rad}}^i}{\sum_i W_i}, \quad (16)$$

and the final radiative stabilization of the product ion after the double-electron transfer (after m steps through the yrast chain) was established as:

$$P_{\text{rad}} = \prod_{k=1}^m P_{\text{rad}}^k. \quad (17)$$

At first, the transferred Rydberg states (n_1, n_2) were calculated based on the ECBM. As the first and the second ionization energies for CO are different [29] (13.99 and 41.25 eV, respectively), the two successive transfers of electrons occur into different levels n_1 and n_2 . For example, for $q = 8$ the difference of the principal quantum number of the transferred levels is expected to be $\Delta n = n_1 - n_2 = 2$, while, for $q = 26$, $\Delta n = 5$. For these transferred states (n_1, n_2) , calculations of the radiative stabilization probabilities were performed, and in Fig. 5 are shown the results obtained. Except at $q = 8, 9, 16, 17$, and 23 , large discrepancies between the measured and calculated data are seen [calculations for $q = 11-14$ were not performed, as for these electron configurations of the projectile (core configurations $1s^2 \dots 4d^6 - 1s^2 \dots 4d^3$) the number of terms necessary to be calculated exceeded our computer capacity]. We have noted a strong dependence of the autoionization decay rates on the transferred levels (n_1, n_2) .

Table I gives radiative and autoionization transition rates for the configurations created after two-electron transfer into levels $n_1 = 12$ and $n_2 = 9$ of the primary ion I^{22+} , predicted by the ECBM, and for the modified configurations with the transferred levels $n_1 = 13$ and $n_2 = 8$. The radiative and autoionization decay rates were obtained in the following ways:

TABLE I. The radiative stabilization probabilities during the cascades of the projectile I^{22+} ion with the core electron configuration $(1s^2..4p)$ after the two-electron-transfer process into the levels $(n_1=12, n_2=9)$, predicted by the ECBM and the modified new levels $(n_1=13, n_2=8)$. The average radiative (A_r) and autoionization (A_a) decay rates for a given configuration were obtained according to Eq. (18) (see text).

Transferred levels: $(n_1=12, n_2=9)$ —ECBM				Transferred levels: $(n_1=13, n_2=8)$ —modified			
Configuration [core+ $(n_1l_1;n_2l_2)$]	A_r (10^{10} s^{-1})	A_a (10^{13} s^{-1})	P_{rad}^k	Configuration [core+ $(n_1l_1;n_2l_2)$]	A_r (10^{10} s^{-1})	A_a (10^{13} s^{-1})	P_{rad}^k
12o; 9l	3.9	142.0	0.05	13q; 8k	7.0	0.3	0.21
12o; 8k	7.0	3.5	0.13	13q; 7i	16.4	0.2	0.22
12o; 7i	16.4	2.9	0.10	13q; 6h	37.0	5.2×10^{-4}	0.98
12o; 6h	37.0	3.0×10^{-3}	0.91	13q; 5g	116.0	9.0×10^{-7}	0.99
12o; 5g	116.0	1.59×10^{-5}	0.99	13q; 4f	16.6	7.9×10^{-5}	0.99
12o; 4f	16.6	6.37×10^{-4}	0.96	13q; 4d	15.9	7.8×10^{-5}	0.90
12o; 4d	15.9	5.5×10^{-4}	0.86				
$P_{\text{rad}}=5.5 \times 10^{-4}$				$P_{\text{rad}}=0.041$			

$$A_r = \frac{\sum_i W_i A_r^i}{\sum_i W_i}, \quad A_a = \frac{\sum_i W_i A_a^i}{\sum_i W_i}. \quad (18)$$

It should be noted that the ECBM can provide only a crude estimation of the transferred levels n_1 and n_2 , which are not so accurate, in particular for partially ionized ions such as those in the present investigations but may contain some uncertainties (the ECBM treats the transferred levels not as integers but as real numbers), and also may change during collisions through additional interactions (see Sec. I). In the present cases the uncertainties of about $\Delta n_1=0.3-0.5$ and $\Delta n_2=0.2-0.4$ are expected for the charge state of the projectiles $8 \leq q \leq 26$. Furthermore, a post-collisional mechanism [7] was incorporated, in which n_2 decreases (by unity), while n_1 increases, from these values of (n_1, n_2) predicted by the ECBM. On the other hand, such changes of the initial (n_1, n_2) configurations can also be supported by the observed mechanism of the correlated double-electron capture [8] where the repulsive interaction between the transferred electrons enhances the difference between the transferred levels. For such new modified (n_1, n_2) configurations of the projectiles, the radiative stabilization was calculated, and is shown in Fig. 6. Surprisingly good agreement in the general behavior of the measured and calculated dependences of P_{rad} in the whole investigated region of the charge state of the projectile is seen, except for that at $q=10$. In these calculations, as in the model described above, only the autoionization decay channels with the highest probabilities are considered; the calculated radiative stabilization ratios should correspond to the minimum value. The present calculations clearly show, as indicated in Table I, that, in the investigated region of the charge state of the projectile, the initially populated levels, rather than the core electron configuration, play a dominant role in the radiative stabilization.

Most of the modified transferred levels (except for $q=8, 17, \text{ and } 24$) differ in their n values only by unity ($\Delta n_1=1$ and $\Delta n_2=-1$) or are the same as those predicted by the

ECBM, indicating once more that the ECBM, which is a purely classical picture of the collisions not including effects such as the repulsive interaction between the transferred electrons, for example, is a reasonably good tool in investigations of low energy, highly charged ion-atom-molecule collisions. In particular, a large difference in the ionization energies of the electrons to be transferred (in the present CO case, about 27 eV), and the small velocity of the projectile, seems to satisfy very well a basic assumption of the ECBM, e.g., a successive transfer of target electrons into the projectile.

Contrary to such processes, in simultaneous transfer of two electrons, the electrons cross over the barrier separating the colliding centers at the same time or very close in time. In such regions around the top of the barrier, e.g., near a saddle point, the Coulomb repulsive interaction between these electrons starts to dominate in the total interactions, resulting in large asymmetries of the transferred levels. This can be more likely in fast collisions and/or for targets with a small difference in the ionization energies of the transferred electrons.

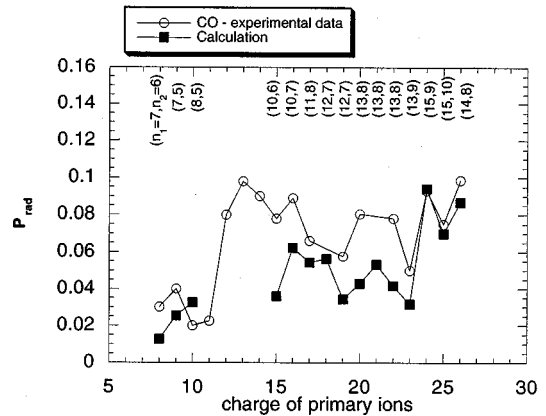


FIG. 6. A comparison of the measured P_{rad} and calculated P_{rad} for the modified transferred levels (n_1, n_2) . The principal quantum numbers for two transferred electrons (n_1, n_2) are shown in the figure.

V. CONCLUSION

We have presented a measurement of the radiative stabilization after double-electron-transfer processes in $1.5q$ -keV $I^{q+} + \text{CO}$ collisions in the charge-state regime $8 \leq q \leq 26$. It is found that the stabilization probabilities P_{rad} generally increase, though some observed structures, as the charge state of the projectile increases. Furthermore there is practically no difference in P_{rad} whether the targets are molecules or atoms. A model is proposed which describes quite well such a feature of P_{rad} , based on the assumption that the electron transfer dominantly occurs into levels with the highest possible l . Consequently, the autoionization decay probabilities for such high- l states cannot take their maximum value, due to the selection rule. This is the reason why the radiative stabilization increases. According to the proposed model, the radiative and autoionization decay rates have been calculated using the Cowan code. The calculations show the very strong dependence of the autoionization decay rates on the transferred levels (n_1, n_2) . This result is not in strong disagreement with the conclusion that the projectile core configuration is more important for the radiative stabilization, as formulated by Cederquist *et al.* [10]; in that experiment in the q region of the projectile, the outer electrons of the core configuration belong to different shells, as opposed to the

present case. For most of the cases where calculations were performed, including the transferred levels predicted by the ECBM, a significant disagreement between the observed and calculated results is observed. By incorporating effects of the correlated electron capture such as the repulsive interaction between the transferred electrons, the calculated P_{rad} for the modified configurations, which still are almost within uncertainties of the transferred levels predicted by the ECBM, have been found to be in very good agreement with the measured data. The fact that most of these new modified (n_1, n_2) levels differ in their values by unity ($\Delta n_1 = 1$ and $\Delta n_2 = -1$), or are the same as those predicted by the ECBM, seems to support the present conclusion that in slow collisions the successive transfer of target electrons into the projectile with small correlation effects between the transferred electrons is dominant, contrary to simultaneous transfer of two electrons, where strong correlation effects are expected to result in a large asymmetry of the occupied levels.

ACKNOWLEDGMENTS

We wish to thank Bob Cowan and Yuri Ralchenko for their help in using Cowan's code, and Andrzej Warczak for helpful suggestions.

-
- [1] R. Ali, C. L. Cocke, M. L. A. Raphaelian, and M. Stöckli, *Phys. Rev. A* **49**, 3586 (1994).
- [2] A. Bárány, G. Astner, H. Cederquist, H. Danared, S. Huldt, P. Hvelplund, A. Johnson, H. Knudsen, L. Liljeby, and K.-G. Rensfelt, *Nucl. Instrum. Methods Phys. Res. B* **9**, 397 (1985).
- [3] M. Barat and P. Roncin, *J. Phys. B* **25**, 2205 (1992).
- [4] N. Vaeck and J. E. Hansen, *J. Phys. B* **25**, 3267 (1992); **26**, 2977 (1993).
- [5] Z. Chen and C. D. Lin, *J. Phys. B* **26**, 957 (1993).
- [6] M. N. Gaboriaud, P. Roncin, and M. Barat, *J. Phys. B* **26**, L303 (1993).
- [7] H. Bachau, P. Roncin, and C. Harel, *J. Phys. B* **25**, L109 (1992).
- [8] N. Stolterfoht, C. C. Havener, R. A. Phaneuf, J. K. Swenson, S. M. Shafroth, and F. W. Meyer, *Phys. Rev. Lett.* **57**, 74 (1986).
- [9] E. Luc-Koenig and J. Bauche, *J. Phys. B* **23**, 1763 (1990).
- [10] H. Cederquist, H. Andersson, E. Beebe, C. Biedermann, L. Broström, Å. Engström, H. Gao, R. Hutton, J. C. Levin, L. Liljeby, M. Pajek, T. Quinteros, N. Selberg, and P. Sigray, *Phys. Rev. A* **46**, 2592 (1992).
- [11] R. Ali, C. L. Cocke, M. L. A. Raphaelian, and M. Stöckli, *J. Phys. B* **26**, L177 (1993).
- [12] I. Ben-Itzhak, S. G. Ginther, V. Krishnamurthi, and K. D. Carnes, *Phys. Rev. A* **51**, 391 (1995).
- [13] A. Remscheid, B. A. Huber, M. Pykavyj, V. Staemmler, and K. Wiesemann, *J. Phys. B* **29**, 515 (1996).
- [14] I. Yamada, F. J. Currell, A. Danjo, M. Kimura, A. Matsumoto, N. Nakamura, S. Ohtani, H. A. Sakaue, M. Sakurai, H. Tawara, H. Watanabe, and M. Yoshino, *J. Phys. B* **28**, L9 (1995).
- [15] Y. Kaneko, T. Iwai, S. Ohtani, N. Kobayashi, S. Tsurubuchi, M. Kimura, and H. Tawara, *J. Phys. B* **14**, 881 (1981).
- [16] W. C. Wiley and I. H. McLaren, *Rev. Sci. Instrum.* **26**, 1150 (1955).
- [17] J. Vancura and V. O. Kostroun, *Phys. Rev. A* **49**, 321 (1994).
- [18] I. Ben-Itzhak, S. G. Ginther, and K. D. Carnes, *Phys. Rev. A* **47**, 2827 (1993).
- [19] K. Hosaka, H. Tawara, I. Yamada, H. A. Sakaue, F. Krok, F. J. Currell, N. Nakamura, S. Ohtani, H. Watanabe, A. Danjo, M. Kimura, A. Matsumoto, M. Sakurai, and M. Yoshino, *Phys. Scr.* **T73**, 273 (1997).
- [20] N. Nakamura, F. J. Currell, A. Danjo, M. Kimura, A. Matsumoto, S. Ohtani, H. A. Sakaue, M. Sakurai, H. Tawara, H. Watanabe, I. Yamada, and M. Yoshino, *J. Phys. B* **28**, 2959 (1995).
- [21] H. A. Sakaue (unpublished).
- [22] H. Andersson, G. Astner, and H. Cederquist, *J. Phys. B* **21**, L187 (1988).
- [23] R. K. Janev, R. A. Phaneuf, and H. Tawara, *At. Data Nucl. Data Tables* **25**, 201 (1993).
- [24] N. Tushima and H. Tawara, *NIFS-DATA-26* (National Institute for Fusion Science, Toki, Japan, 1997).
- [25] W. Fritsch and C. D. Lin, *Phys. Rev. A* **29**, 3039 (1984).
- [26] I. Yu. Tolstikhina, Ph.D. thesis, The Graduate University for Advanced Studies, Nagoya, 1996 (unpublished).
- [27] A. I. Akhiezer and V. B. Berestetsky, *Quantum Electrodynamics* (Nauka, Moscow, 1959).
- [28] R. D. Cowan, *The Theory of Atomic Structure and Spectra* (University of California Press, Berkeley, 1981).
- [29] V. Krishnamurthi, K. Nagesha, V. R. Marathe, and D. Mathur, *Phys. Rev. A* **44**, 5460 (1991).